Review on Design of Frequency Selective Surfaces based on Substrate Integrated Waveguide Technology

Krushna Kanth Varikuntla[1], Raghavan Singaravelu[2]

[1,2]Department of Electronics and Communication Engineering,
National Institute of Technology Trichy,
Tiruchirappalli, TN, India
*corresponding author, E-mail: krushnakanthv@gmail.com

Abstract

The spectacular development of frequency selective surfaces (FSS) as a spatial filter, absorbers and reflectors made them feasible for the aerospace and defence applications. The intervention of substrate integrated waveguide (SIW) technology into FSS results in the improvement of unit cell structures and better performance by isolating them from inter-element interference. Such FSS structures with SIW cavities upholds the FSS properties and improves their selectivity and performance. Considering the diversity in applications of introducing SIW cavity technology into FSS, the aim of this paper is to furnish a study on the glimpse of EM design techniques to analyze this type of structures. Design topologies of narrowing bandwidth, dual resonance, the design of FSS with sharp sideband edges and frequency selective polarization rotating structures are presented. Further, a novel design for improving the bandwidth of reflective FSS is discussed based on SIW technology. Fabrication techniques pertaining to this type of structures are presented in brief.

Keywords: Dual band FSS, equivalent circuit, frequency selective surfaces, substrate integrated waveguide, loaded FSS, lumped element, microwave propagation, quarter mode SIW, polarization rotator.

1. Introduction

Frequency selective surfaces (FSS) are periodic structures either in 2D or 3D, popularly used in the spatial filtering of electromagnetic (EM) waves. A numerous FSS elements such as loops, centre connected, and the combination of both have been proposed for facilitating the required pass-band and stop-band characteristics [1-8]. These structures possess their potential applications in the area of aerospace, sub-reflectors of the antenna, WLAN, wireless security in a communication system, RCS reduction, radar, radar absorbers and radome design etc. [9-14].

A conventional reflect/transit FSS arrays may be placed in/on the building walls to avoid the interference and signal leakage with nearest localities. An undesirable behaviour may occur when conventional FSS elements used as a band-pass filter in building walls, it may accept some higher order resonant frequencies [15], [16]. Furthermore, a unit cell size of FSS at low frequency is higher, leads to instability and degrades the performance when the size of wall is smaller than the wavelength. It is expected to provide a stable resonance at different impinging of EM waves with wall structure, but that is not obtained using conventional FSS. To address this problem a loaded lumped elements in FSS is proposed [17], [18]. By this approach, a miniaturized dimension smaller than a wavelength can be obtained for a single unit cell. All these techniques are based on an assumption of no interference among the unit cells of FSS array. But, in reality, the behaviour of conventional FSS array is not matching with predicted performance [19]. A wide variety of designs and strategies were addressed in open literature for improving the performance characteristics of conventional FSSs. Active FSSs, fractal FSSs, metamaterial inspired FSSs, FSS based on SIW technology are few techniques used in literature.

The Faraday cage structure is well-known design, it has the advantage of providing good isolation in electromagnetic energy for different components designed on same substrate material [20], [21]. It consists a chain of grounded metallic cylinders with a defined diameter (vias) placed at equidistance, encircling sensitive and noisy components in a chip. The via technology features high aspect ratio, through substrate holes filled with copper (Cu) by electrolysis process [22]. A similar Faraday cage has been used to design a loaded FSSs using SIW technology with help of FDTD method [23]. The SIW cavity FSS technique first applied to design a band-pass filter [24]. As of late, a lot of work has published on SIW technology into FSS design [25]-[27]. An elaborated study has been done on controlling the bandwidth of FSS using SIW technology [28], [29].

FSS with sharp transition sidebands at lower and higher frequencies can be achieved by slightly adjusting the coupling magnitude between two resonances. This performance, therefore, to get an FSS with two different SIW cavities cascading and shunting [30], [31]. The SIW structure upholds the advantages of conventional rectangular waveguides, such as high-quality factor, selectivity, directivity, cut-off frequency characteristics and high power handling etc. [32]-[34]. The well-developed form of polarization rotating surfaces with added advantages of SIW have been reported in the open literature [39]-[41]. Based on the orientation of outgoing wave, the polarization rotators

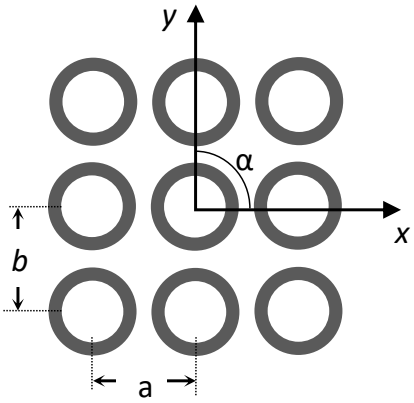

Figure 1. Arrangement of basic FSS elements.

can be classified as a reflection type and transmitting type. The detailed design methodology of polarization rotator is explained in further sections. Many design structures of FSS elements based on SIW reported in the literature are dealing only with slot elements. The SIW technology for patch type FSS elements is not reported so far. In this paper, an attempt has been made to develop patch type FSS based on SIW technology.

The description of FSS elements is briefed in section 2. Whereas the main topic of interest, design methods and topologies of FSSs using SIW technology is explained in section 3. In section 4, few designed models of this kind of structures are presented. The fabrication techniques pertaining to this structures are explicated in section 5. Finally, the topic is concluded in section 6.

2. Design of FSS Elements

The conventional FSS is placed along its axis, supported by the dielectric a 2-D or 3-D planar periodic array of the patch (reflective) or slot (transitive) elements substrate. A typical square arrangements (α=90º) is shown in figure 1. The performance of an FSS is often attributed entirely to the elements [1], [4].

Many techniques and structural topologies have been proposed to design FSS elements. The unusual behaviour of FSS elements due to larger dimensions at higher frequencies is mentioned in the previous section. To overcome this limitation, FSS using SIW cavity is adopted. The EM design techniques of this kind of structures are described in further sections.

3. EM Design Techniques and Analysis of FSS using SIW

Many methods have been adopted to analyze the scattering characteristics of FSS such as equivalent circuit model (ECM) [2, 5, 7], method of moments (MoM) [41, 42], FDTD and spectral domain techniques [24]. These techniques are efficient in their own way to solve the planar infinite periodic surfaces. The glimpse of these methods is discussed in this section.

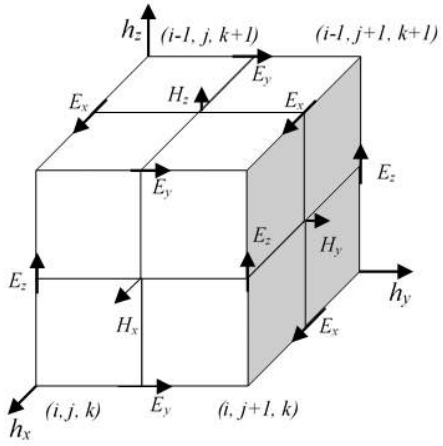

Figure 2. Yee cell model of an element with 3-D nonuniform meshes.

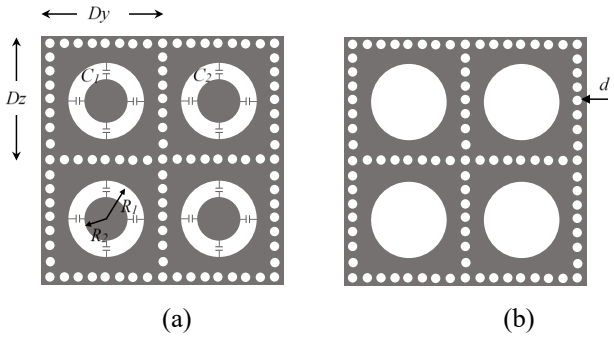

Figure 3. Arrangement of basic FSS elements: (a). Front view, (b) Back view

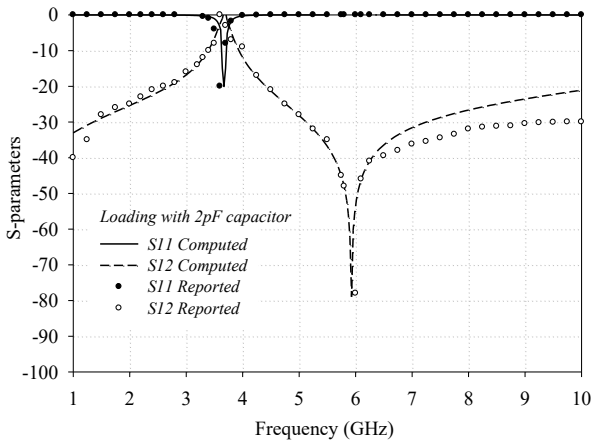

Figure 4. S-parameters loaded FSS with SIW. Solid line show computed result at dept. of ECE, NITT. Bubbles show reported results from figure 2 [23].

3.1. FDTD Method

The finite difference time domain (FDTD) is partial differential equation based method. It is formulated by discretizing Maxwell's curl equations and approximating the derivatives to the difference equations. The Yee FDTD algorithm can be applied on a distributed grid is as shown in figure 2. It is well suited for modelling perfect electric conductor (PEC) boundary conditions. *E*- and *H*- field components are aligned at centre in three-dimensional space. As a result every *E*- field component is surrounded by four *H*-field components and every *H*- field component surrounded by four *E*- field components [35], [36]. This method instantly approximates the differential operators in the Maxwell curl equations, on a grid staggered in time and space. *E*- and *H*-fields are computed on a regular grid with field components being offset by $\Delta s/2$ relative to each other and *E*- and *H*-fields evaluated $\Delta t/2$ apart in time, here Δs and Δt are the spatial and temporal discretization values respectively. This permits a scheme which uses first-order numerical differentiation to provide second order accuracy. It is also the only widely used computational electromagnetic technique to be operated in the time domain.

A topology of FSS having two neighbouring loaded capacitive ring slot resonators, each neighbouring unit determines a passband is shown in figure 3. The undesirable coupling between FSS elements is suppressed by Faraday cage structure created by a row of metallic vias connecting both top and bottom PEC planes as discussed earlier. As a result, independent design of passbands is possible. The necessary conditions to create a Faraday cage for better isolation performance are $d \geq 0.5k$ and $d \leq 0.1\lambda_0$. The described loaded FSS topology is validated and compared in figure 4 with the reported results.

The computation can also solve the lumped elements (RLC) by inserting into the FDTD lattice, thus Maxwell's curl equation for H-field becomes [36].

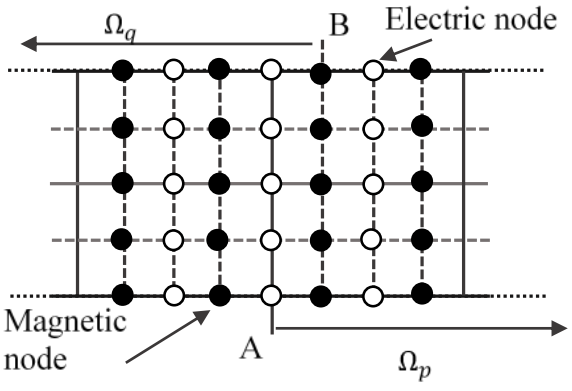

Figure 5. Electric and magnetic field nodes at virtual boundary.

$$\nabla \times \vec{H} = \frac{\partial \vec{D}}{\partial t} + \vec{J}_{resistance} + \vec{J}_{capacitance} + \vec{J}_{inductance} \quad (1)$$

The problem domain is truncated by using Mur's absorbing boundary conditions (ABC). The detailed formulation of fields and absorbing boundary representations are represented in [24]. The equations further used to compute the electric field density *D,* the transformed field equations for *D* components do not change [16]. This method is well suitable for simple and planar periodic FSS incorporated SIW structures [23]. The influences of various parameters on the frequency response of FSS based on SIW cavity can be estimated. The FDTD method is easy and simple for modelling the structure with loaded lumped elements. The method is formulated by discretizing Maxwells's curl equations, finally approximating the derivatives with difference equations.

3.2. FDTD Combined with Domain Decomposition Method

The computational complexity is drastically increased for multilayer structures by using FDTD method. Hence, the finite difference frequency domain (FDFD) combined with domain decomposition method (DDM) been used to solve the large-scale computation of cascading cavity FSS and to reduce the CPU computational time [25]. In this method, whole problem domain is decomposed into $m = l + 2$ non-overlapping subdomains, where l is a number of SIW cavities. From figure 5, let Ω_q is one of these subdomains, $\Gamma_{p,q} = \Omega_q \cap \Omega_p$ denotes interface between Ω_q, Ω_p. Total problem domain thus split into *m* small problem and field equations at virtual interface $\Gamma_{p,q}$ can be calculated by applying virtual boundary condition (VBC). Through the VBC, each sub domain can exchange information with neighboring subdomain. The DDM combined with FDFD can be useful to compute the transmission characteristics of cascaded SIW cavity FSS. The memory required for computation thus reduced from N to N/m, where N is the total unknowns of the structure [25].

3.3. Equivalent Circuit Model

The EC model is simple design technique to analyze any microwave circuit. This model will not consider all *EM* effects and losses associated with the structure. But, it can give a knowledge of parametric effect on the response of a structure with an initial approximation. The FSS using SIW structure can be modelled with a lumped element circuit, which can consist of two coupled parallel resonators. The equivalent circuit representation is shown in figure 6. In cascading SIW cavity FSS, the preliminary work is to find out the dimension of coupling slots between SIW cavities when single SIW cavity FSS dimensions are known to design. The lumped elements in the circuit can be estimated by applying dual-mode filter and coupling matrix theory The circuit optimization thus applied to determine optimal coupling parameter in FSS with two or more cascaded SIW

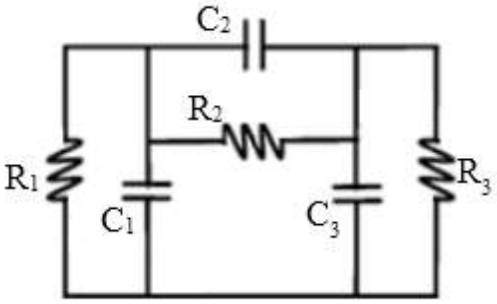

(a)

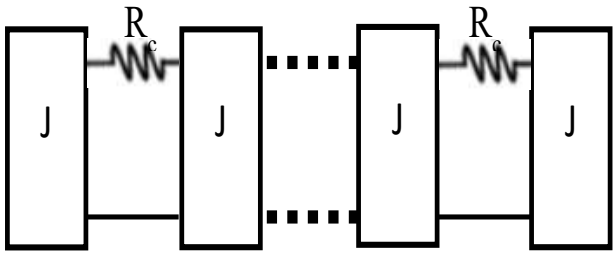

(b)

Figure 6. Equivalent circuits: (a) Single SIW cavity FSS J. (b) Cascading SIW cavity FSS.

cavities. With the given lumped element parameters and geometrical parameters of SIW cavity FSS, the frequency responses of an FSS with an arbitrary number of cascading SIW cavities can be calculated. It is also possible to study the frequency responses of the structure *w.r.to* different angles of incidence and polarization [25].

3.4. MoM/Bi-RME Method

Method of moment (MoM) boundary integrated-resonant mode expansion (BI-RME) method was originally developed to model an inductive and capacitive FSS [41], [42], afterwards applied to the modelling of boxed microstrip circuits and electromagnetic band gap (EBG) structures [43]. This method is much faster than commercial *EM* simulators. For reducing structural complexity and computational time, SIW cavity is modelled as a standard waveguide based on the basic waveguide equations of SIW. SIW cavity is the main element designed in this method, its resonant frequency for TM_{mn} mode is given in Equation (2) [41]:

$$f_r = \frac{c_0}{2\sqrt{\varepsilon_r}}\sqrt{\left(\frac{m}{W_{eff}}\right)^2 + \left(\frac{n}{L_{eff}}\right)^2} \quad (2)$$

where

$$W_{eff} = W - \frac{D^2}{0.95b} \text{ and } L_{eff} = L - \frac{D^2}{0.95b} \quad (3a)$$

these equations are valid for

$$b < \frac{\lambda_0\sqrt{\varepsilon_r}}{2} \text{ and } b < 4D \quad (3b)$$

Here D represents the diameter of SIW vias, b is their distance, W and L correspond to the length and width of cavity respectively.

However, many design techniques has been adopted to analyze the frequency and phase response of FSS elements. A mutual impedance method, modal matching method and EC methods are extensively used to analyze the performance of FSS [1, 44]. At first the FDTD, MoM and spectral domain techniques are applied to FSS by Kieburtz [45]. Point matching method has been discussed for analysis of FSS [46].

4. FSS Structures Using SOW Topology

The designed structures using above techniques are showing their potential applications in specific area s. A few designed structures are presented in this section proposed in the earlier literature for specific applications.

4.1. Design of Double Square loop FSS-SIW Cavity

The geometry of unit cell of the dual-band FSS with SIW cavity is shown in figure 7. A double square loop (DSL) FSSs are symmetrically etched on top and bottom PEC surfaces of substrate material. Conventional FSS is a single conducting screen with double slots perforated on top and bottom planes, each unit cell is thus isolated with SIW cage [27]. The proposed structure is validated by taking the mentioned parameters and a comparison has been made in figure 8, with computed results to the originally reported results.

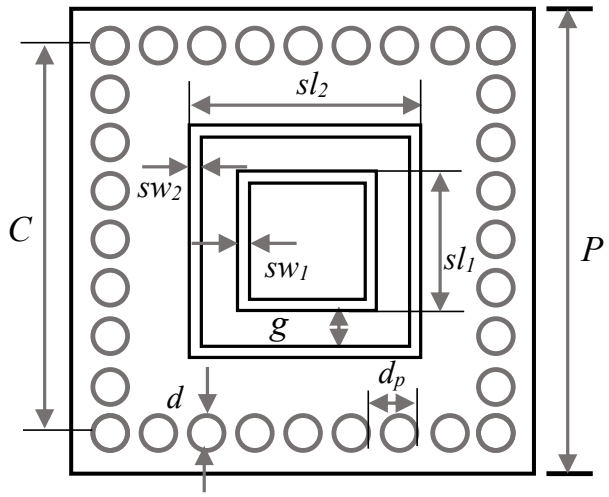

Figure 7. Dual band configuration of SIW–cavity using Double Square loop FSSs (design parameters are referred from [27]).

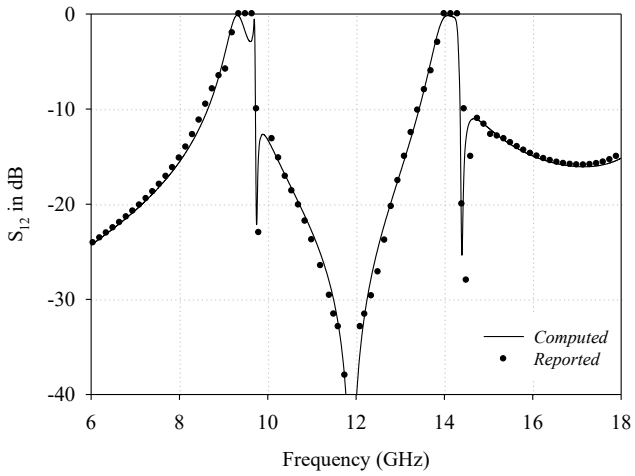

Figure 8. Transmission coefficient of SIW–cavity using Double Square loop FSSs. Solid line show computed result at dept. of ECE, NITT. Bubbles show reported results from figure 2 in [27].

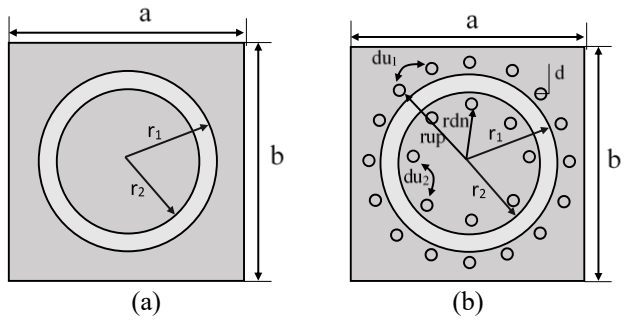

Figure 9. Unit cell configuration of FSS: (a) Ring aperture FSS. (b). SIW cavity ring aperture FSS (design parameters are referred from [28]).

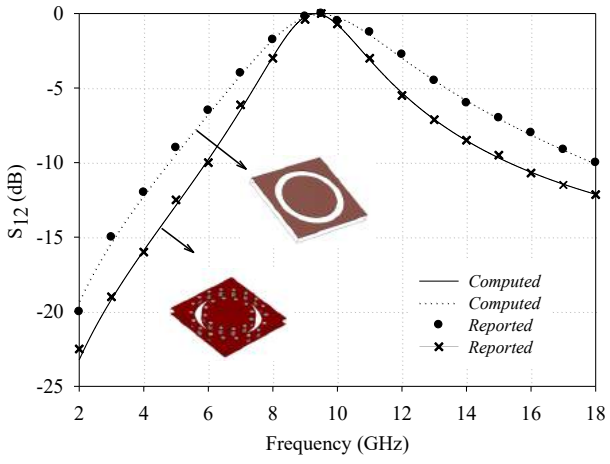

Figure 10. Transmission coefficient of FSS and SIW cavity FSSs. Solid and dotted lines show computed results at dept. of ECE, NITT. Bubbles and cross show reported results from Figure 4.a in [28].

4.2. Reducing the Bandwidth of FSS using SIW

A method of reducing the bandwidth of FSS for higher frequency selectivity is demonstrated with an experiment using SIW cavity technology [28]. The resonance in frequency happens only when the perimeter of the loop slot is a multiple of wavelength (λ) regardless the shape of FSS element [1], [4], [38]. The intervention of SIW into FSS element does nothing with the shape of ring element. Hence, the centre frequency remains unchanged. The design conventional FSS element and modified SIW cavity FSS is presented figure 9. The structural dimensions are referred to [28].

SIW technology introduced into the design of FSS brings in the parallel inductance in the equivalent circuit. As a result, the equivalent inductance increases in the circuit. According to the following equations:

$$Q = \frac{2\pi f_0 L}{R} \tag{4}$$

$$f_0 = \frac{1}{2\pi\sqrt{LC}} \tag{5}$$

where f_0 is resonant frequency *R, L, C,* are resistance, inductance, and capacitance of the *EC* model respectively. From the Equation (4) and (5) it is clear that Q is directly proportional to inductance (*L).* Hence, bandwidth is narrower, and the proposed new topology of FSS has a higher selectivity than conventional FSS element. The novel design of FSS [28] is validated and compared the results in figure 10.

4.3. FSS using Quarter mode SIW

An FSS based on quarter mode SIW (QMSIW) has been reported, to provide two controllable poles with in the pass-band and a sharp roll off at one side of the pass-band. The structure is depicted in figure 11. In this topology, single mode SIW with FSS will exhibit polarization rotation characteristics. Stable frequency response in the passband can be achieved by this structure [39]-[40]. By repeating this structure along with it centre, QMSIW can be derived. To design a QMSIW with FSS, following conditions should satisfy 1. QMSIW cavity can be applied to the periodic topology, 2. Coupling structure should not have the polarization selectivity, and 3. The FSS element has more than two resonant modes to optimize the passband. The resonant frequency (f_c) of the QMSIW cavity is given as [21]:

$$f_c = \frac{c_0}{\sqrt{2\varepsilon_r}} \times \left(\frac{1}{2 \cdot sl_2} \right) \tag{5a}$$

The resonant frequency (f_s) of the *L*-type slot is depended on length of slot, hence it should be long enough to make f_s near to f_c of the fundamental mode in QMSIW cavity, and be approximately equal to half wavelength. The f_s is expressed as:

$$f_s = \frac{c_0}{\sqrt{\varepsilon_{eff}}} \times \left[\frac{1}{2(sl_1 + sl_2)} \right] \tag{5b}$$

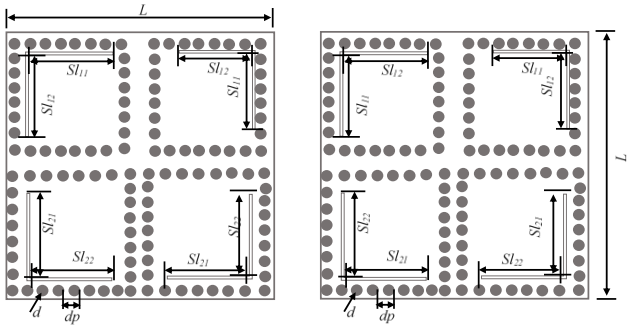

(a) (b)

Figure 11. Multiband configuration of QMSIW–FSS. (a) Top layer. (b) Bottom layer.

Where sl_1 and sl_2 are the lengths of the *L*-type slot. ε_{eff} is the effective dielectric constant of the substrate material, which is equal to $(\varepsilon_r + 1)/2$.

4.4. Frequency Selective Polarization Rotator Based on SIW

Polarization rotation of impinging EM wave on a planar surface is a profound application of FSS. An FSS element based on SIW technology shows a superior performance for polarization rotation structure [39]-[41]. Based on the direction of wave propagation, these surfaces are broadly classified as reflective and transitive polarization rotators. Transmission type structures contain a slotted coupled elements are etched on one side of the substrate and at the other end, elements are etched with 90° to facilitate rotation EM wave. The wave impinges on the top surfaces can pass through the slots and permutate in the SIW cavity. Finally, at another end, a rotated EM wave can found because of the twisted slots. The design example is shown in figure 12a. Whereas, the reflective type structure, one end is completely shorted with metal. The impinging wave passes through the slots and permutated in the SIW cavity. The wave reflected back through the slots offers a polarization rotation. An example structure for reflective type is shown in figure 12b.

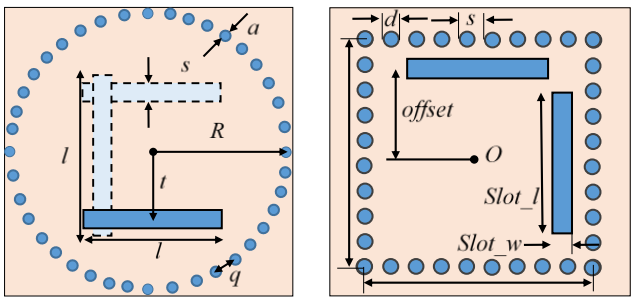

(a) (b)

Figure 12. Unit cell topology of Polarization rotators. (a) Transmission type [40]. (b) Reflective type [39].

4.5. Design of FSS Based on SIW with Sharp side band Characteristics

The spectacular applications of FSS as polarizers, space filters, etc., are mainly limited because of its poor selectivity and susceptibility to the change in polarization state and incidence angle. Many techniques such as multilayered configurations, stacked photonic bandgap structures have been discussed open literature. However, some applications needed high selectivity performance from FSS. The conventional multilayered FSS makes them bulky and unsuitable for practical use. In this regard, FSS realized with shunting and cascading SIW cavities have been reported for two sharp sideband response [31].

a. Cascading: The cascaded structure of crossed dipoles with different sizes is shown in figure 13.a. The top and bottom layers identical shapes with different cavity couplings. Whereas the width of the middle layer a slightly higher than the front end. The period of all elements is same. The coupling of two different size cavities results in obtaining two passbands with sharp sidebands. The frequency response of the same structure is shown in figure 13.c.

b. Shunting: The fabrication of cascaded FSS with SIW cavities is quite a difficult process. Hence, the shunting of two structures is addressed with similar performance characteristics. The two structures with different cavities can shunt as shown in figure 13.b. The top and bottom shapes of the structure are identical. The design parameters of both structures are referred from [31].

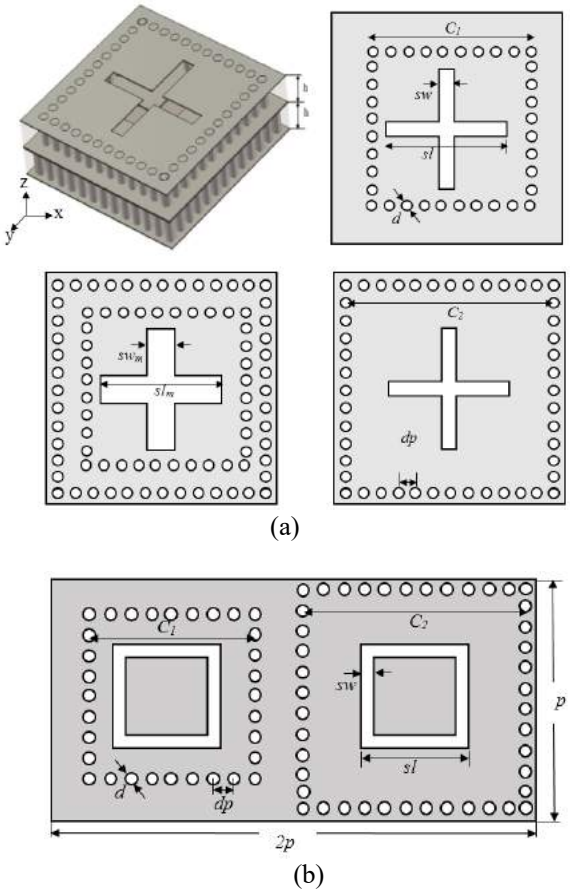

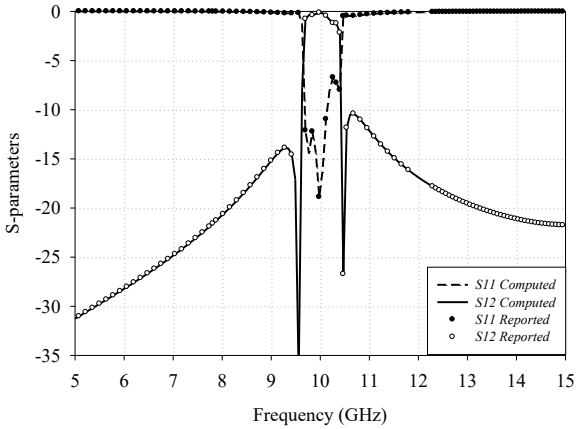

(c)

Figure 13. FSS design for sharp side band response based on SIW. (a) Cascading, (b) Shunting, (c) frequency response. Dashed and Solid lines show computed results at dept. of ECE, NITT. Bubbles show the reported results from Figure 3 in [31].

4.6. Improving the Bandwidth of FSS using SIW

Till date, FSS designs based on SIW are dealing with slot type elements only. SIW technology is not reported for patch type FSS elements. The patch FSS elements act as an EM reflectors which can found their enormous applications in the design reflector surfaces, antenna substrates including the design of radar absorbing structures (RAS), high-impedance surfaces (HIS). However, the bandwidth of patch elements is a major limitation for many practical applications. 3-D FSS may offer wideband but the high thickness makes then not feasible for many practical applications. Also, the power handling capabilities of conventional elements are poor and lose their basic performance characteristics at high microwave power levels due to break down (chapter 10. [1]). To address the above-mentioned limitations of conventional FSS, in this section, a novel form of SIW technology is applied to the patch FSSs. Figure 14 shows the design of proposed FSS element configuration from the conventional form (fig. 14a-c) and its frequency response (fig. 14d). The design parameters of the structure are: p = 14 mm, l = 6.35, w = 1 mm and thickness of the substrate is 1.57 mm. A dielectric substrate material Rogers RT 5880 ($\varepsilon_r = 2.2$ and $\tan\delta = 0.0009$) has been used for the analysis. The ECM representation of conventional tripole FSS is shown in Figure 14b. Where L and C represents the equivalent inductance and capacitance respectively, which are expressed by equation 6 and 7:

$$X_L = \omega L = \frac{l}{p} F(p, 2s, \lambda, \theta) \tag{6a}$$

$$B_C = \omega C = 4\frac{l}{p} F(p, g, \lambda, \theta) \times \varepsilon_{eff} \tag{6b}$$

In the expression, l is the length of tripole leg, and g is the gap beween two adjecent lelenets ($\approx p$-l). λ and θ are the free space wavelength and incidence angle respectively.

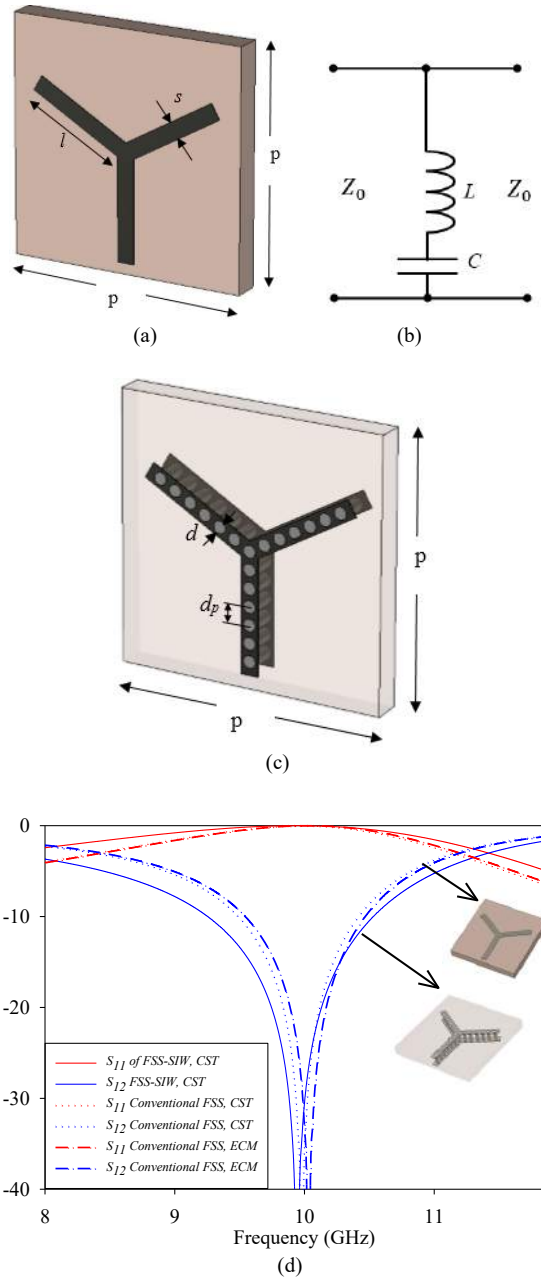

Figure 14. Tripole FSS unit cell. (a) Conventional form, and its (b) equivalent circuit model, (b) Proposed form. (c) Comparison of frequency response.

Where,

$$F(p, w, \lambda, \theta) = \frac{p}{\lambda}\cos\theta\left\{\ln\left(\csc\left(\frac{\pi w}{2p}\right) + G(p, w, \lambda, \theta)\right)\right\} \tag{7a}$$

$$G(p, w, \lambda, \theta) = \frac{0.5\left[\left(1-\alpha^2\right)^2\left\{\left(1-0.25\alpha^4\right)\cdot\left(A_- + A_+\right) + \left(4\alpha^2 A_- A_+\right)\right\}\right]}{\left[\left(1-\frac{\alpha^2}{4}\right) + \alpha^2\left(1+\frac{\alpha^2}{2}-\frac{\alpha^4}{8}\right)\cdot\left(A_- + A_+\right) + \left(2\alpha^6 A_- A_+\right)\right]} \tag{7b}$$

$$A_{\mp} = \frac{1}{\sqrt{1 \mp \left(2p\sin\theta/\lambda\right) - \left(p\cos\theta/\lambda\right)^2}} - 1 \tag{7c}$$

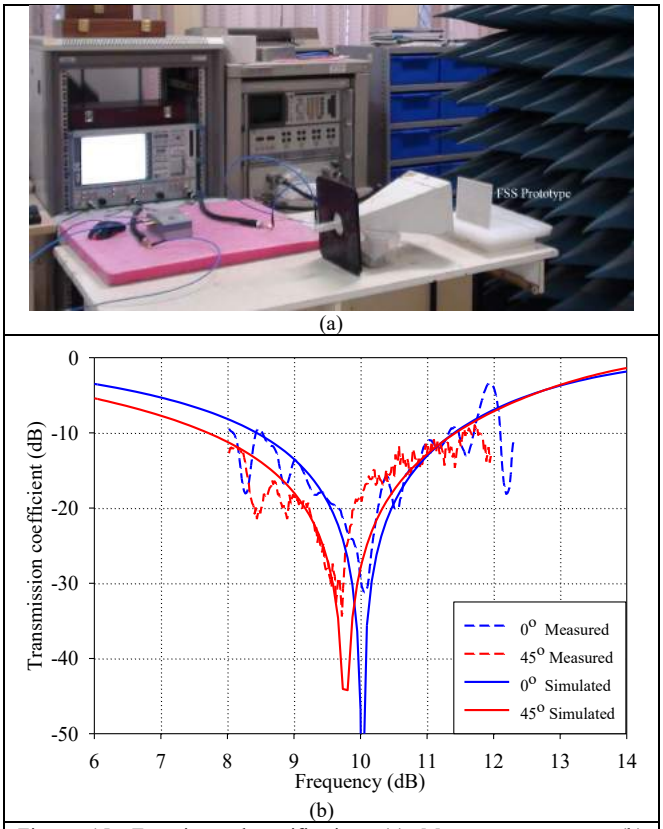

Figure 15. Experimental verification, (a) Measurement setup, (b) Comparison of simulated and measured results at normal and 45° incidence angle.

$$\alpha = \sin(\pi w/2p). \tag{7d}$$

Then, the total impedance offered by the equivalent circuit is expresses in equation 8.

$$X_g = j\left(\omega L - \frac{1}{\omega C}\right) \tag{8}$$

The transmission coefficient expressed as:

$$|\tau|^2 = \frac{4|X_g|^2}{1+4|X_g|^2} \tag{9}$$

Figure 14b shows the comparison of simulated results of ECM and CST MWS for conventional form. The results show the agreement between both methods. Further, the proposed structure has been simulated using simulation tool. Next, the metallic vias have been created on the patch element. The design results in virtually thick FSS screen and offers an improvement in its bandwidth. From the frequency response comparison shown in figure 14d, it is observed that the reflection bandwidth (-10 dB) of the structure is improved from 0.92 GHz to 1.4 GHz. Moreover, the design can offer many advantages over conventional form. Because of the two screens printed on either side of substrate and metallic via results in better EM field distribution across the element. Hence, results in better performance at high power levels. In addition, it can overcome the limitations of 3-D FSS screens. The 3-D FSS elements can be designed using the proposed design with reduced weights. The simulation of the proposed element has been performed on the FDTD based commercial EM simulator CST microwave studio. The periodic boundaries have been applied along the x and y direction. Whereas, Floquet mode excitation is applied on the z-direction as a source.

Figure 15 shows the experimental verification of fabricated prototype discussed above. The 10 × 10 array has been fabricates using conventional PCB with designed dimensions. A single port method has been used to characterize the sample. A standard gain X- band (8.2 GHz - 12.4 GHz) horn antenna has been used as a testing antenna. The comparison shows the good agreement between simulated and measured results. Hence, prove the efficacy of estimated results.

5. Fabrication Method

The technological design aspects of SIW structures show their significance at millimetre-wave frequency range and at a very high-frequency range (> 40 GHz). Commercially printed circuit board (PCB) techniques have been widely adopted to fabricate SIW structures, due to its simple design process, less complexity and low cost. In this method, metal vias are created by either micro-drilling or laser etching. Finally, their metallization thus performed by electroplating (or by using copper paste) [47]. The advantage of PCB technique is, possible to realize an entire circuit including a transition, planar circuitry, waveguide components and devices in a single board [48]. As the frequency increases the LTCC technology can be used for SIW implementation. By using this technology multiple layers with tiny dimensions and extreme ultrathin SIW structures can be implemented [49]-[51].

6. Conclusions

This paper has presented the glimpse of design techniques and applications of FSS based on SIW cavity technology: this includes recent advances in the field of spatial filtering, and FSS design using SIW cavity technology. Issues pertaining to the analysis, design, and modelling techniques are briefly explained. Further, few design examples of FSS elements based on SIW technology is presented for different applications. Also, a novel vias technique to uphold the FSS properties with increasing BW is discussed. The technique can be applied to all kind of patch FSS elements to create virtually thick screens. Fabrication methods pertaining to this kind of structures have been addressed.

Acknowledgements

Authors are thankful to Dr. D. C. Pande, Distinguished fellow, LRDE-DRDO, Bangalore for his timely suggestions and technical discussions.

References

[1] B. A Munk, *Frequency selective surfaces: Theory and design*, Wiley, New York, 2000.

[2] R. J. Langley, E. A. Parker, Equivalent circuit model for arrays of square loops, *Electronics Letters*, Vol. 18, no. 7, pp. 294-296, 1 April 1982.

[3] T. S. MOK and E. A. PARKER, Gridded square frequency-selective surfaces, *International J. of Electronics*, Vol. 61, no. 2, pp. 219-224, 24 8 1986.

[4] R. Orta, P. Savi and R. Tascone, The Effect of Finite Conductivity on Frequency Selective Surface Behavior, *J. of Electromagnetics*, Vol. 10, no. 3, pp. 213-227, 7 1990.

[5] R. J. Langley, A. J. Drinkwater, Improved empirical model for the Jerusalem cross, *IEE Proc*. Vol. 129, no. 1, pp. 1-6, February 1982.

[6] J. C. Vardaxoglou, E. A. Parker, Performance of two tripole arrays as frequency-selective surfaces, *Electronics Letters*, Vol. 19, no. 18, pp. 709-710, 1st September 1983.

[7] C. K. Lee, R. J. Langley, Equivalent-circuit models for frequency selective surfaces at oblique angle of incidence, *IEE Proc*., Vol. 132, no. 6, pp. 395-399, February 1982.

[8] Y. Yang, H. Zhou, X.-H. Wang and Y. Mi, Low-pass frequency selective surface with wideband high-stop response for shipboard radar, *J. of Electromagnetic Waves and Applications*, Vol. 27, no. 1, pp. 117-122, jan. 2013.

[9] B. A. Munk, *Finite Antenna Arrays and FSS*: Wiley, New York, 2003.

[10] W.-T. Wang, S.-X. Gong, X. Wang, H.-W. Yuan, J. Ling and T.-T. Wan, RCS Reduction of Array Antenna by Using Bandstop FSS Reflector, *J. of Electromagnetic Waves and Applications*, Vol. 23, no. 11-12, pp. 1505-1514, Jan. 2009.

[11] P. Kong, X. Yu, M. Zhao, Y. He, L. Miao and J. Jiang, Switchable frequency selective surfaces absorber/reflector for wideband applications, *J. of Electromagnetic Waves and Applications*, Vol. 29, no. 11, pp. 1473-1485, Jul. 2015.

[12] C. de Lucena Nóbrega, M. Ribeiro da Silva, P. H. da Fonseca Silva and A. G. D'Assunção, Analysis and design of frequency selective surfaces using teragon patch elements for WLAN applications, *J. of Electromagnetic Waves and Applications*, Vol. 28, no. 11, pp. 1282-1292, jul. 2014

[13] P. Kim, D. Lee, I. Seo and G. Kim, Low-observable radomes composed of composite sandwich constructions and frequency selective surfaces, *Composites Science and Technology*, Vol. 68, no. 9, pp. 2163-2170, Jul. 2008.

[14] R. U. Nair and R. M. Jha, Electromagnetic Design and Performance Analysis of Airborne Radomes: Trends and Perspectives [Antenna Applications Corner], *IEEE Antennas and Propagation Magazine*, Vol. 56, no. 4, pp. 276-298, Aug. 2014.

[15] E. A. Parkar, et al., Application of FSS structure to selectively control the propagation of signals into and out of buildings, *Tech. Rep. AY4464, ERA Technology Ltd*., 2005.

[16] R. R. Xu, H. C. Zhao, Z. Y. Zong and W. Wu, Dual-Band Capacitive Loaded Frequency Selective Surfaces With Close Band Spacing, *IEEE Microwave and Wireless Components Letters*, Vol. 18, no. 12, pp. 782-784, Dec. 2008.

[17] K. Sarabandi and N. Behdad, A Frequency Selective Surface With Miniaturized Elements, *IEEE Trans. on Antennas and Propagation*, Vol. 55, no. 5, pp. 1239-1245, May 2007.

[18] F. Bayatpur and K. Sarabandi, Single-Layer High-Order Miniaturized-Element Frequency-Selective Surfaces, *IEEE Trans. on Microwave Theory and Techniques*, Vol. 56, no. 4, pp. 774-781, April 2008.

[19] S. M. Amjadi and M. Soleimani, Narrow Band-Pass Waveguide Filter Using Frequency Selective Surfaces Loaded with Surface Mount Capacitors, 2007 International Conference on Electromagnetics, *Advanced Applications*, Torino, pp. 173-176, 2007.

[20] K. Joardar, Comparison of SOI and junction isolation for substrate crosstalk suppression in mixed mode integrated circuits, *Electronics Letters*, Vol. 31, no. 15, pp. 1230-1231, Jul 1995.

[21] H. B. Wang and Y. J. Cheng, Frequency Selective Surface With Miniaturized Elements Based on Quarter-Mode Substrate Integrated Waveguide Cavity With Two Poles, *IEEE Trans. on Antennas and Propagation*, Vol. 64, no. 3, pp. 914-922, March 2016.

[22] J. H. Wu, J. Scholvin, J. A. del Alamo and K. A. Jenkins, A Faraday cage isolation structure for substrate crosstalk suppression, *IEEE Microwave and Wireless Components Letters*, Vol. 11, no. 10, pp. 410-412, Oct. 2001.

[23] R. R. Xu, H. C. Zhao, Z. Y. Zong and W. Wu, Loaded frequency selective surfaces using substrate integrated waveguide technology, *Microwave and optical technology letters*, Vol. 50, no. 12, pp. 3149-3152, Dec. 2008.

[24] G. Q. Luo et al., Theory and experiment of novel frequency selective surface based on substrate integrated waveguide technology, *IEEE Trans. on Antennas and Propagation*, Vol. 53, no. 12, pp. 4035-4043, Dec. 2005.

[25] G. Q. Luo, W. Hong, H. J. Tang and K. Wu, High Performance Frequency Selective Surface Using Cascading Substrate Integrated Waveguide Cavities, *IEEE Microwave and Wireless Components Letters*, Vol. 16, no. 12, pp. 648-650, Dec. 2006.

[26] G. Q. Luo et al., Filtenna Consisting of Horn Antenna and Substrate Integrated Waveguide Cavity FSS, *IEEE Trans. on Antennas and Propagation*, Vol. 55, no. 1, pp. 92-98, Jan. 2007.

[27] G. Q. Luo, W. Hong, H. J. Tang and K. Wu, Dualband frequency-selective surface using substrate integrated waveguide technology, *IET Microwave and Antenna propagation*, Vol. 1, no. 2, pp. 408-413, April 2007.

[28] N. N. Qi, S. X. Gong, Y. J. Zhang, and J. F. Liu, Reducing bandwidth of FSS using substrate integrated waveguide technology, *J. of Electromagnetic waves and applications,* Vol. 22, no. , pp. 2087-2096, 2008.

[29] H. Zhou, S. Qu, Z. Pei, J. Zhang, B. Lin, J. Wang, H. Ma and C. Gu, Narrowband frequency selective surface based on substrate integrated waveguide

technology, *Progress In Electromagnetics Research Letters,* Vol. 22, no. , pp. 19-28, March 2011.

[30] P. Kong, X. Yu, M. Zhao, Y. He, L. Miao and J. Jiang, Switchable frequency selective surfaces absorber/reflector for wideband applications, *J. of Electromagnetic Waves and Applications,* Vol. 29, no. 11, pp. 1473-1485, 24 7 2015.

[31] G. Q. Luo, W. Hong, Q. H. Lai and L. L. Sun, Frequency –selective surfaces with two sharp sidebands realized by cascading and shunting substrate integrated waveguide cavities, *IET microwave Antenna propagation*, Vol. 2, no. 1, pp 23-27, February 2008.

[32] Y. Cassivi, L. Perregrini, P. Arcioni, M. Bressan, K. Wu and G. Conciauro, Dispersion characteristics of substrate integrated rectangular waveguide, *IEEE Microwave and Wireless Components Letters*, Vol. 12, no. 9, pp. 333-335, Sept. 2002.

[33] V.V.S. Prakash, S. Christopher, A Selective Survey of the Waveguide-Fed Slot Radiators, *IETE Technical Review*, Vol. 17. nos. 1&2, pp. 51-59, April 2000.

[34] P. Kong, X. Yu, M. Zhao, Y. He, L. Miao and J. Jiang, Switchable frequency selective surfaces absorber/reflector for wideband applications, *J. of Electromagnetic Waves and Applications*, Vol. 29, no. 11, pp. 1473-1485, 24 7 2015.

[35] Shiv Narayan, K. M. Divya, V. Krushna Kanth, *FDTD Modeling of EM Field inside Microwave Cavities*, Springer Nature, 2017.

[36] D.M. Sullivan, *Electromagnetic Simulation using the FDTD Method*, IEEE Press, 2000.

[37] M. Piket-May, A. Taflove and J. Baron, FD-TD modeling of digital signal propagation in 3-D circuits with passive and active loads, *IEEE Trans. on Microwave Theory and Techniques*, Vol. 42, no. 8, pp. 1514-1523, Aug 1994.

[38] N. N. Qi, S. X. Gong, P. F. Zhang, J. F. Liu, A novel Y-loop aperture frequency selective surface using substrate-integrated waveguide technology, *Microwave and Optical Technology Letters,* Vol. 50, no. 12, pp. 3023-3027, Dec. 2008.

[39] X. C. Zhu, W. Hong and K. Wu, H. J. Tang, Z. C. Hao, J. X. Chen, G. Q. Yang, A Novel Reflective Surface With Polarization Rotation Characteristic, *IEEE Antennas and Wireless Propagation Letters,* Vol. 12, pp. 968-971, 2013.

[40] M. S. M. Mollaei,Narrowband Configurable Polarization Rotator Using Frequency Selective Surface Based on Circular Substrate-Integrated Waveguide Cavity, *IEEE Antennas And Wireless Propagation Letters*, Vol. 16, pp. 1923-1926, Mar. 2017

[41] S. A. Winkler, W. Hong, M. Bozzi, and k. Wu, polarization rotating frequency selective surface Based on substrate integrated waveguide technology, *IEEE Trans. on Antennas and Propagation,* Vol. 58, no. 4, april 2010.

[42] M. Bozzi, L. Perregrini, J. Weinzierl, and C. Winnewisser, Efficient analysis of quasi-optical filters by a hybrid MoM/BI-RME method, *IEEE Trans. Antennas Propag*., vol. 49, no. 7, pp. 1054–1064, Jul. 2001.

[43] M. Bozzi and L. Perregrini, Analysis of multilayered printed frequency selective surfaces by the MoM/BI-RME method, *IEEE Trans. Antennas Propag*., vol. 51, no. 10, pp. 2830–2836, Oct. 2003.

[44] Chao-Chun Chen, Scattering by a two-dimensional periodic array of conducting plates, *IEEE Transactions on Antennas and Propagation*, vol. 18, no. 5, pp. 660-665, Sep 1970.

[45] R. Kieburtz and A. Ishimaru, Scattering by a periodically apertured conducting screen, *IRE Transactions on Antennas and Propagation*, vol. 9, no. 6, pp. 506-514, November 1961.

[46] R. H. Ott, R. G. Kouyoumjian and L. Peters, Scattering by a two-dimensional periodic array of narrow plates, *Radio Science*, vol. 2, no. 11, pp. 1347-1359, Nov. 1967.

[47] Bozzi, M., A. Georgiadis, and K. Wu., Review of substrate-integrated waveguide circuits and antennas, *IET Microwaves Antennas & Propagation,* Vol. 5, no. 8, pp. 909-920, 2011.

[48] K. Wu, Towards system-on-substrate approach for future millimetre wave and photonic wave application, *Proceeding of Asia-pacific microwave conference,* 2006

[49] Yu Wang, Jianming Zhou, Yinqiao Li and Xiao Yang, Design of a Ka-band dual-mode filter based on LTCC technology, 2015 *IEEE 6th International Symposium on Microwave, Antenna, Propagation, and EMC Technologies (MAPE)*, Shanghai, 2015, pp. 604-607.

[50] H. Chu, Y. X. Guo, Y. L. Song and Z. L. Wang, 40/50 GHz diplexer design in LTCC technology, *Electronics Letters*, Vol. 47, no. 4, pp. 260-262, February 17 2011.

[51] B. J. Chen, T. M. Shem and R. B. Wu, Dual-band Vertically Stacked Laminated Waveguide filter Design in LTCC Technology, *IEEE Trans. on Microwave Theory and Techniques*, Vol. 57, no. 6, pp. 1554-1562, Jun. 2009.